Photonics Breakthroughs 2024: Multidimensional Integrated (de)Multiplexers for Optical Fiber Communications

Xianyi Feng, Wu Zhou, *Graduate Student Member, IEEE*, Hao Chen, *Graduate Student Member, IEEE*, Yuzhe Ma, *Member, IEEE*, and Yeyu Tong, *Member, IEEE*

***Abstract*—The growing demand for higher data transmission capacity, particularly driven by advancements in artificial intelligence and cloud computing, has spurred the exploration of various degrees of freedom (DoF) of light in optical communication systems, including wavelength, polarization, and spatial modes. Consequently, multidimensional optical multiplexing has emerged as a pivotal enabling technology. However, the development of compact, cost-effective, and scalable multidimensional optical interconnects remains a significant challenge. In this work, we present our recently demonstrated ultra-compact multiplexer fabricated on silicon, capable of selectively launching eight spatial and polarization modes into a few-mode optical fiber with a footprint of less than $35 \times 35\ \mu\mathrm{m}^2$. The corresponding peak experimental coupling efficiencies for linearly polarized (LP) modes $\mathrm{LP}_{01-x/y}$, $\mathrm{LP}_{11a-x/y}$, $\mathrm{LP}_{11b-x/y}$, and $\mathrm{LP}_{21b-x/y}$ are -3.8 dB, -5.5 dB, -3.6 dB, and -4.1 dB, respectively. Compared with previous approaches, our device facilitates the selective excitation of different LP modes in an ultra compact manner, while preserving polarization diversity and competitive coupling efficiencies. Additionally, we review recent advancements in multidimensional optical multiplexing based on photonic integrated circuits. We also address the principal challenges associated with our proposed methodologies and discuss future directions, including strategies for enhancement and potential applications.**

***Index Terms*—Optical fiber communications, integrated optics, optical multiplexing, silicon photonics, spatial-division multiplexing, polarization-division multiplexing.**

I. Introduction

THE relentless surge in data-driven technologies, including artificial intelligence and cloud computing, has placed unprecedented demands on communication capacity and bandwidth density in optical communication systems. There is a pressing need to aggregate more data lanes while within a minimized form factor. Although dense-wavelength-division multiplexing (DWDM) has been extensively deployed in modern long-haul optical fiber communication networks, mirroring its success into the cost- and power-sensitive short-reach communications becomes very challenging, particularly in the integration of optics onto boards and within packages [1], [2], [3]. Scaling the number of wavelength channels is often constrained by its reliance on high-performance laser sources, as well as the limited optical bandwidth of all the involved optical or optoelectronic components.

Researchers have thus turned to leveraging additional degrees of freedom (DoF) of light, including orthogonal polarizations and spatial modes, which is also known as polarization-division multiplexing (PDM) and mode-division multiplexing (MDM). The exploration of multiple closely-spaced fiber cores has also been undertaken. As a result, spatial-division multiplexing (SDM) optical fibers can be broadly categorized into multi-core fiber (MCF), few-mode fiber (FMF), and multi-mode fiber (MMF) [4], [5], [6]. Owing to the reduced operation complexity, limited supported modes, and minimized intermodal dispersion, FMFs and multi-core FMFs have recently demonstrated record-high communication capacities [7], [8], [9]. However, in contrast to advancements in the wavelength domain, integrating polarization and mode dimensions into a communication system in a compact, cost-effective, and energy-efficient manner remains a significant challenge.

Enabled by the rapid advancements in approaches such as multi-plate light conversion (MPLC) [10], [11], metasurfaces [12], [13], fiber photonic lanterns [14], and laser-inscribed three-dimensional waveguides [15], selectively launching of orthogonal spatial modes with a minimal insertion loss and channel crosstalk becomes achievable. However, the deployment of bulky free-space optics often necessitates precise alignment and assembly processes. The required serial manufacturing techniques may also impose constraints on fabrication costs and scalability. In addition, the inevitable crosstalk that arises following demultiplexing process presents another significant concern. While this issue can be solved through coherent receivers and digital signal processing (DSP) electronics, the resulting power consumption and latency are often prohibitive for short-reach interconnects [16], [17], [18]. An example is the chip-to-chip interconnect, which demands ultra-high data throughput while simultaneously adhering to

Received 28 February 2025; revised 12 May 2025; accepted 14 May 2025. Date of publication 16 May 2025; date of current version 30 May 2025. This work was supported in part by the National Natural Science Foundation of China under Grant 62305277, in part by the Natural Science Foundation of Guangdong Province under Grant 2024A1515012438, in part by Nansha District Key Area S&T Scheme under Grant 2024ZD007, and in part by the Guangzhou Association for Science and Technology under Grant QT2024-011. *(Corresponding author: Yeyu Tong.)*

The authors are with the Microelectronics Thrust, Hong Kong University of Science and Technology (Guangzhou), Guangzhou 511453, China (e-mail: xfeng262@connect.hkust-gz.edu.cn; wzhou832@connect.hkust-gz.edu.cn; hchen390@connect.hkust-gz.edu.cn; yuzhema@hkust-gz.edu.cn; yeyutong@hkust-gz.edu.cn).

Digital Object Identifier 10.1109/JPHOT.2025.3570958

stringent requirements for energy efficiency and cost per bit.

Leveraging the high refractive index contrast and utilizing CMOS-compatible fabrication methods, silicon photonics facilitates the development of highly compact planar photonic integrated circuits (PICs) on silicon-on-insulator (SOI) substrates [19], [20], [21], [22], [23]. Consequently, one of earliest efforts focused on the development of diffraction grating couplers on chip as mode multiplexers for FMFs. When combined with heater-based optical phase shifters, these systems facilitate the development of higher-order spatial beam generators via a nano-grating antenna-based optical phase array [24], [25], [26], [27], [28], [29]. To further incorporate polarization diversity, 2D grating coupler (2DGC) based antenna was employed [30], [31], [32], [33], [34], [35]. By applying push-pull control of intensity and phase to each diffraction antenna, 2DGC array can launch higher-order mode while supporting polarization diversity [36], [37], [38], [39]. Different from the fixed spatial distribution after emission, a four-arm 2DGC was first proposed to coherently launch TE_0 and TE_1 modes in counter directions [40]. Although various linearly-polarized (LP) fiber modes including LP_{01}, LP_{11a}, LP_{11b}, or even LP_{21b} in dual polarizations can be excited, their reported efficiencies were typically below -20 dB which necessitates new design strategy. Through incorporation of effective medium theory (EMT) and optimization algorithm, 2D grating coupler supporting four LP modes with experimental efficiencies about -6.1 dB was first demonstrated [41]. Apart from that, a 2DGC array featuring four small-feature-size blazed grating structures capable of generating six LP modes has demonstrated efficiencies of -5.2 dB for LP_{01} and -9 dB for LP_{11} modes [34], [42].

Edge couplers, another widely deployed chip-to-fiber I/O solution, have also been investigated to address the dimensionality limitations [44], [45], [46], [47], [47], [48], [49]. Through the integration of asymmetric directional couplers (ADCs) [50], mode-evolution couplers [51], and polarization beam rotators (PBRs) [52] for comprehensive multidimensional on-chip manipulation [48], optimized edge coupler between FMF and PIC offer potential advantages including much wider optical bandwidth and coupling efficiencies. However, mitigating the mode-field mismatch between SOI waveguides and FMF is even more difficult than the case of standard single-mode fibers, typically requiring additional fabrication processes including multi-layer deposition [47], [53], three-dimensional silica waveguide attachment [46], [54]. To avoid the significant field distribution mismatch between PIC and circular-core FMFs, rectangular-core FMFs and tapered FMF have been proposed [45], [47], [49].

Although selective excitation of various spatial and polarization modes have been demonstrated via integrated photonic I/O components, they exhibit certain performance limitations including insufficient excitation efficiency and limited number of spatial or polarization channels. In this paper, Section II presents our recent results achieved for compact and multidimensional chip-to-fiber I/O. Our design can increase the number of spatial and polarization channels to eight LP modes for a four-mode FMF, while achieving an ultra-compact footprint and high coupling efficiency. Section II-B offers an overview of other relevant studies on multidimensional optical chip-to-fiber I/O solutions and chip-to-chip communications published in 2024. Section III addresses current limitations and future directions, concluding with a discussion of the potential impact of our results.

II. Breakthrough Research

To enable a multidimensional I/O interface while in an ultra compact manner, we proposed and demonstrated a 2D grating coupler on SOI with subwavelength spot size converters (SSCs). Up to eight LP modes including $LP_{01-x/y}$, $LP_{11a-x/y}$, $LP_{11b-x/y}$, and $LP_{21b-x/y}$ can be selectively launched while occupying a footprint of only 35×35 μm^2. The measured peak coupling efficiencies for all supported spatial and polarization channel are >-5.5 dB. Our proposed ultra-compact and multi-dimensional I/O design can potentially be used with multi-core FMFs to achieve densely integrated photonic circuits in various SDM applications [43].

A. Concept and Principle

The proposed (de)multiplexer shown in Fig. 1(a) is fabricated on a 220-nm SOI platform with a 2-μm-thick buried oxide. The device consists of a multi-mode grating coupler (MMGC), four SSCs, and four tapered ADCs. Optical signals are initially coupled into eight single-mode waveguides via an optical fiber array using an external laser source. Heater-based phase shifters are employed to dynamically adjust the relative phase of each fundamental TE mode. Tapered ADCs are utilized for on-chip mode de/multiplexing, and converting two fundamental modes to a TE_0/TE_1 pair. The four multiplexed TE_0/TE_1 pairs are then directed into the same 2D grating region. Selective LP mode excitation depends injected waveguide modes and their relative phase difference. As illustrated in Fig. 1(d), the mechanism operates as follows:

- $\mathbf{LP}_{01}$: When in-phase TE_0 modes are injected from opposing directions (e.g., north-south or east-west), constructive interference occurs leading to the formation of a merged quasi-Gaussian beam profile.
- $\mathbf{LP}_{11a}$: Out-of-phase TE_0 modes input from east-west directions can generate a pair of kidneys [55] in x polarization. Alternatively, two in-phase TE_1 modes input from north-south directions can directly excite LP_{11} mode in y polarization.
- $\mathbf{LP}_{11b}$: Owing to the symmetric design of the grating region, LP_{11b} modes are generated analogously to LP_{11a} modes, but in the orthogonal direction.
- $\mathbf{LP}_{21b}$: When out-of-phase TE_1 modes are injected from opposing directions, a quadrupole field pattern can be obtained to two degenerate LP_{21b} modes.

1) MMGC Design: As shown in Fig. 1(b), the proposed MMGC is an optimized 2DGC and consists of shallow-etched circular holes with a 70 nm etch depth and achieves high efficiency for both TE_0 and TE_1 mode in 13 μm-wide slab waveguide. To suppress spatial modes distortion and maintain identical coupling performance for four ports, the grating region requires strict structural symmetry and perfectly vertical

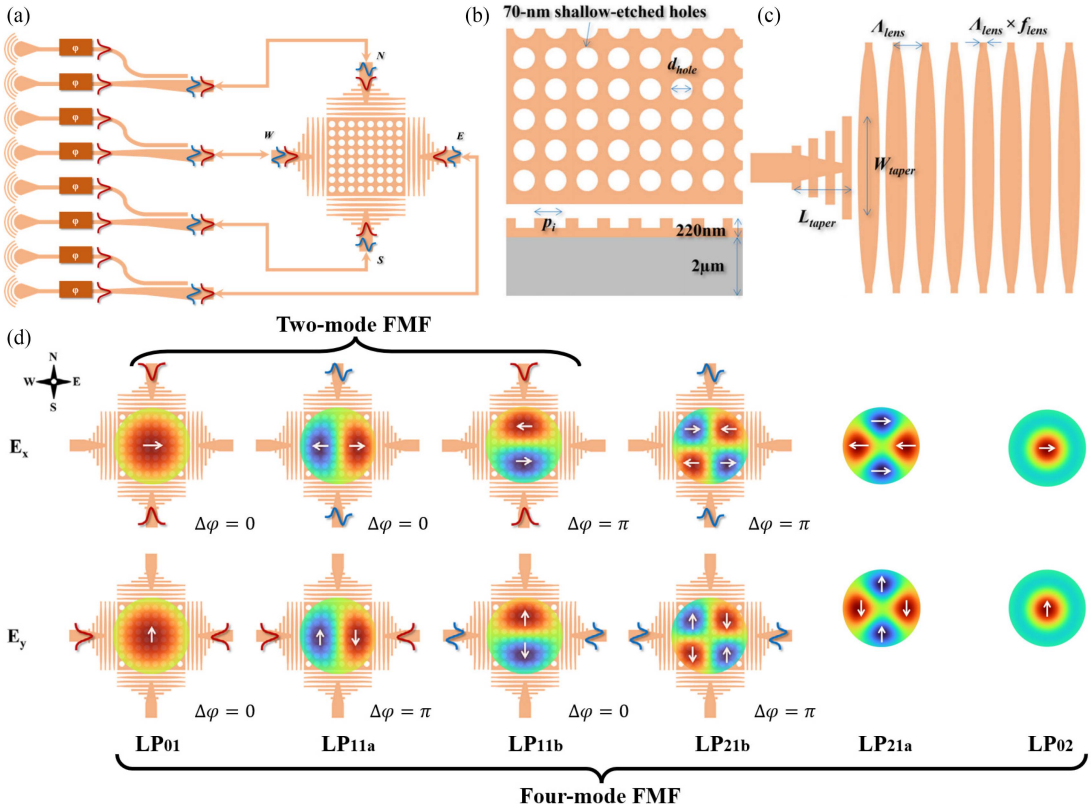

Fig. 1. (a) Schematic illustrations of the integrated multimode (de)multiplexer, which consists of a 2D MMGC, four SSCs, and four ADCs. Eight heater based optical phase shifters are needed for mode multiplexing. A top-down view of the SSCs (b) and MMGC (c) designed for perfectly vertical chip-to-fiber coupling. (d) Schematic illustration of selective mode launching for mode LP_{01}, LP_{11a}, LP_{11b}, and LP_{21b} in an FMF via proposed design [43].

coupling. To address second order Bragg diffraction induced reflection, chirped grating is utilized in our design [56], [57]. To reduce computation complexity in electromagnetic wave simulation, we implement following design workflow to obtain optimized grating parameters:

- The 3D subwavelength structure is mapped into a 2D model by the 2nd-order EMT to approximate the effective index of the grating region.
- Since the effective indices of TE_0 and TE_1 modes are nearly identical in the wide grating waveguide, the coupling efficiency of the fundamental mode is selected as the figure of merit (FOM) to evaluate device performance. Genetic algorithm combined with 2D finite-difference time-domain (FDTD) simulations are employed to optimize the grating parameters [41], attaining an etched hole diameter of 343 nm and grating periods as shown in [43].
- Finally, the optimized parameters are validated in 3D FDTD model to assess the excitation performance across all supported LP modes.

2) Ultra-Compact Spot Size Converter: To avoid the long adiabatic taper waveguide needed for mode size expansion in our design, a compact and mode-independent SSC is crucial. Mikaelian lens, with its aplanatic capability, facilitates both paraxial and nonparaxial light focusing, making it advantageous for higher-order mode beam expansion [22], [23]. Based on EMT, subwavelength structures can be treated as uniform materials with specific effective refractive indices [19], [20], [21]. Integrated Mikaelian lens can achieve a graded effective refractive index profile by spatially varying the duty cycle of the subwavelength structure as depicted in Fig. 1(c). The grating features a pitch of 240 nm and a width of 13 μm, with the duty cycle varying continuously from 0.3 to 0.7. This variation maps the effective refractive index from $n_{\min} = 2.26$ at the edge to $n_{\max} = 3.02$ at the center. A subwavelength taper at the lens input is needed to reduce the insertion loss.

3) Results and Achievements: The results of 3D FDTD simulation are shown in Fig. 2. Mode-independent field size conversion between waveguides with a width of 0.962 μm and 13 μm can be achieved using the subwavelength Mikaelian SSC, showing peak conversion efficiencies of -0.02 and -0.07 dB for the TE0 and TE1 modes, respectively. Meanwhile, the inter-modal crosstalks are below -30 dB across the C-band. Fig. 2(b) shows the coupling spectra of our proposed 2D grating for various x-polarized LP modes. An identical performance for the LP mode in the y polarization can be obtained due to symmetric design. The LP_{01} and LP_{11a} modes exhibit minimum coupling losses of -3.61 and -3.94 dB at 1532 nm, respectively, with a 1-dB bandwidth of approximately 47 nm. The LP_{11b} and LP_{21b} modes show minimum losses of -3.17 and -3.75 dB at 1577 nm, with a 1-dB bandwidth of approximately 35 nm. The mode-dependent loss difference is below 3 dB over a 21 nm spectral range. The peak coupling efficiencies of the four spatial

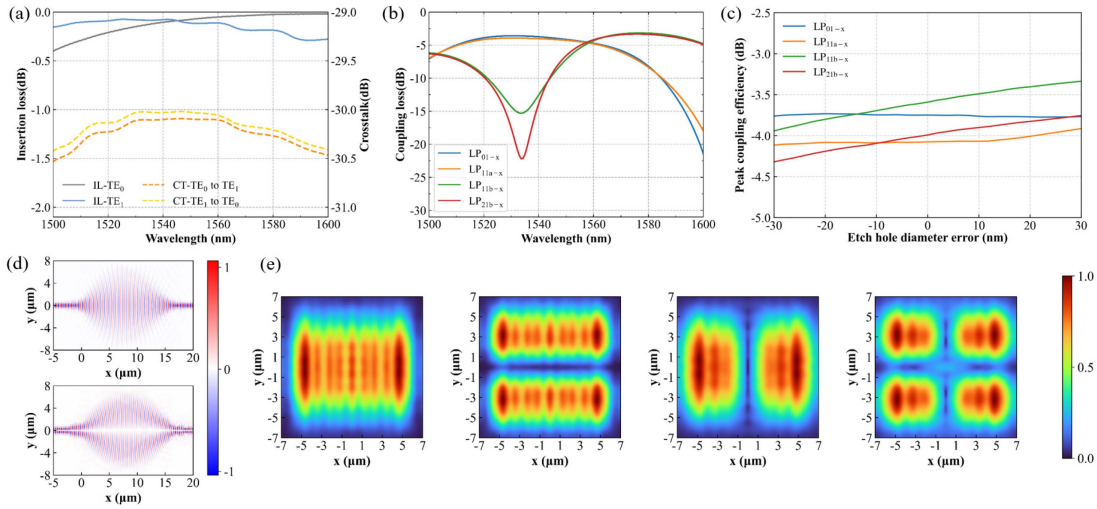

Fig. 2. 3D FDTD simulated results: (a) Transmission spectra and crosstalk of the subwavelength Mikaelian lens for mode field size conversion; (b) Coupling loss spectra for different spatial modes; (c) Peak coupling efficiency variation of different modes with respect to etch hole diameter error; (d) Optical field profiles of the subwavelength Mikaelian lens in a back-to-back configuration for mode size conversion; (e) Diffracted optical intensity profile of the MMGC[43].

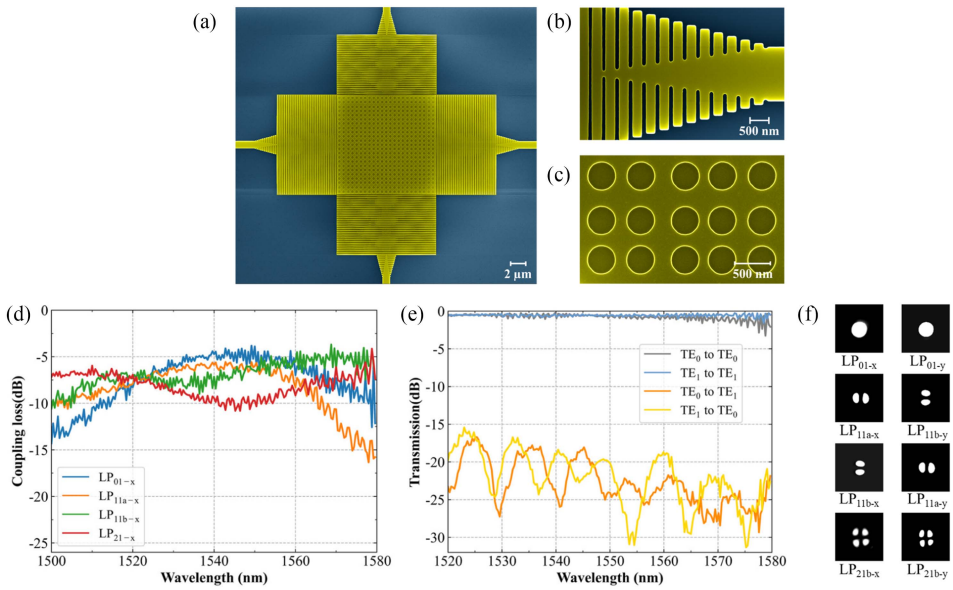

Fig. 3. (a)–(c) Scanning electron microscope (SEM) images of the fabricated MMGC and SSCs. (d) Normalized coupling loss spectra of the MMGC for x-polarized LP_{01}, LP_{11a}, LP_{11b}, and LP_{21b} modes. (e) Measured insertion loss and crosstalk spectra for the subwavelength Mikaelian lens. (f) Intensity profile captured when different modes are selectively launched [43].

channels have a wavelength shift due to the variations in optimal mode overlap integrals when using coherent excitation with controlled phase conditions. Addressing this issue requires the simultaneous consideration of all mode efficiencies during the optimization process.

We further evaluated the fabrication tolerance of the proposed FMGC. As shown in Fig. 2(c), the peak coupling efficiencies of the LP_{01}, LP_{11a}, LP_{11b}, and LP_{21b} modes were analyzed with respect to etch hole diameter errors ranging from –30 nm to +30 nm. All four modes exhibit stable performance, with peak efficiency variations within ±0.5 dB across the tested range, indicating robust performance despite manufacturing imperfections.

Scanning electron microscope (SEM) images of the fabricated MMGC and SSCs are presented in Fig. 3(a)–(c). The total footprint in Fig. 3(a) is only $35\times35\ \mu m^2$. The coupling loss of the MMGC was measured using fiber-chip-fiber transmission with a tunable CW laser source and a power meter. Due to the low insertion loss of the proposed SSC, two and four Mikaelian lenses connected back-to-back are used to obtain the normalized insertion loss and crosstalk shown in Fig. 3(e). Eight LP modes can be selectively launched by adjusting the heater-controlled phase shifters on each input waveguide as shown by the intensity profile in Fig. 3(f) captured by an infrared camera. The overall experimental results shown in Fig. 3(d) demonstrate peak coupling efficiencies of −3.8 dB ($LP_{01-x/y}$),

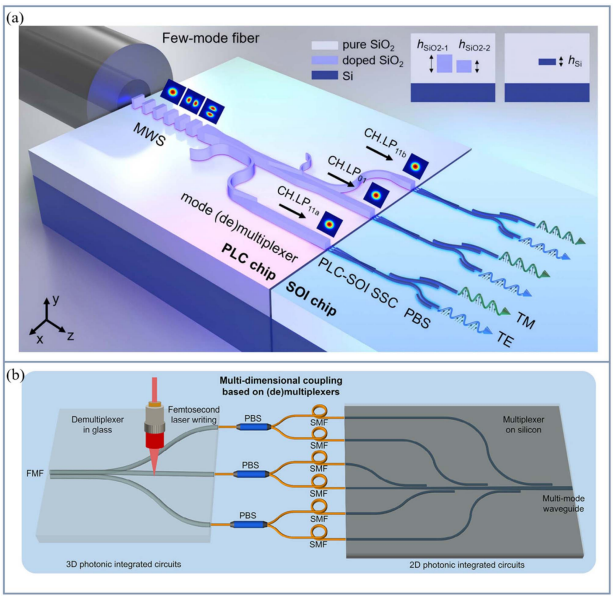

Fig. 4. Edge coupler based multidimensional (de)multiplexer assisted with (a) PLC chip [58] and (b) laser-inscribed 3D waveguide [59].

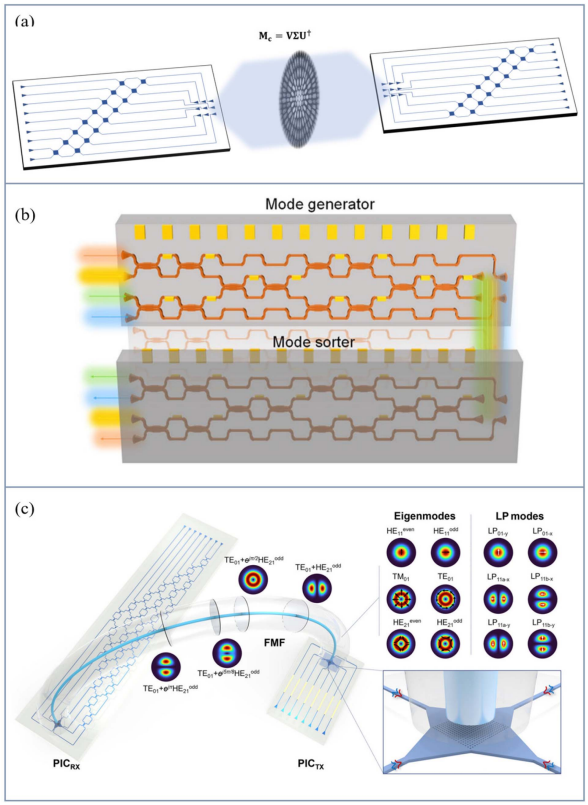

Fig. 5. MZI-based configurable MIMO processor: (a) SVD network for free-space communications, image adapted from ref [61]. (b) Programmable 4×4 network for free-space communications [62]. (c) Photonic processor for chip-to-chip fiber communications [63].

-5.5 dB ($LP_{11a-x/y}$), -3.6 dB ($LP_{11b-x/y}$), and -4.1 dB ($LP_{21b-x/y}$), with mode-dependent loss variation <3 dB over a 21 nm bandwidth. The measured 1-dB spectral bandwidth is approximately 20 nm for all spatial channels, which is narrower than the simulation results. This discrepancy arises because the relative phase shift is optimized only for the center wavelength during the wavelength scan, causing hybrid modes to be excited at the edges of the scanning range.

B. Other Breakthroughs in 2024

1) Multidimensional Chip-to-Fiber I/O: Edge coupler based method potentially presents the advantages of low insertion losses and broad operational bandwidths when the mode mismatch can be mitigated. In order to unlock the high coupling efficiency of edge coupler-based (de)multiplexers, planar silica lightwave circuits (PLC) as an intermediate layer was demonstrated [58], as illustrated in Fig. 4(a). On the PLC platform, multi-segment waveguide structures (MWS) expand mode fields in silica waveguides by gradually transitioning the duty cycle. The LP_{01}, LP_{11a}, and LP_{11b} modes are then extracted using polarization-insensitive mode rotators and asymmetric directional couplers (ADCs), where the rotators convert LP_{11b} to LP_{11a} modes with <0.04 dB excess loss. For PLC-to-SOI butt coupling, triple-tip SSCs adiabatically convert silica waveguide modes to TE_0/TM_0 modes in silicon waveguides, while PBSs separate orthogonal polarizations. Experimentally, this hybrid integration achieves total coupling losses of 1.36 - 2.48 dB for six LP modes across a 150 nm bandwidth. Fig. 4(b) shows a different approach utilizing femtosecond-laser-inscribed 3D silica waveguides with the insertion loss of -12.87 dB for mode field expansion and evolution [59], [60]. By integrating six mode/polarization channels and 16 wavelength channels through micro-ring modulators (MRMs), each transmitting 16 Gbaud QPSK signals, the system achieves a total transmission speed exceeding 3 Tbps.

2) Multidimensional Chip-to-Chip Interconnects: Chip-to-chip multidimensional interconnects require both I/O devices and corresponding MIMO signal processing techniques. MIMO optical signal processors based on reconfigurable PICs have been explored in recent years, offering another promising solution in the optical domain to solve the signal mixing after spatial and polarization demultiplexing [61], [62], [63], [64], [65], [66], [67], [68]. In this context, we will focus on the breakthroughs in 2024 multidimensional chip-to-chip interconnects.

By using a reconfigurable MZI network integrated with a 3×3 1DGC antenna array as shown in Fig. 5(a), chip-to-chip MDM free-space optical communications was achieved without knowing any predetermined optical modes [61]. An intermodal crosstalk below -30 dB for two concurrent channels can be realized in experiment. This solution demonstrates exceptional resilience in scattering media, setting new benchmarks for adaptive optical interconnects. Ref. [62] proposed a chip-to-chip multimode optical communication system using universal mode processors based on a 2×2 1DGC antenna array and a programmable 4×4 MZI network as depicted in Fig. 5(b). Experimental results demonstrated the ability to support LP_{01}, LP_{11a}, LP_{11b}, LP_{21b}, and OAM_0, OAM_1 modes, enabling 25 Gbps data transmission across multiple mode channels.

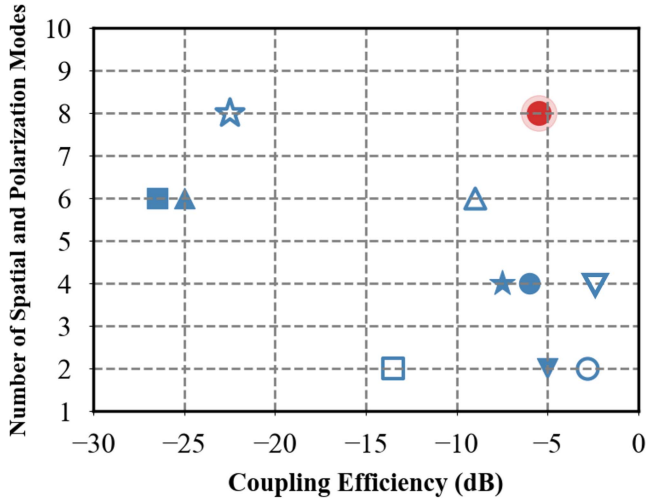

Fig. 6. Comparison of the number of selectively excited spatial and polarization channels and minimum coupling efficiency of integrated multiplexers based on SOI platform [37], [38], [39], [40], [41], [42], [43], [44], [49], [69], [70], where our work is indicated by the red dot.

Since our proposed integrated multiplexer can supported all the spatial and polarization fiber modes in a two-mode FMF as illustrated in Fig. 1(a), we also proposed and demonstrated an integrated photonic processor enabling chip-to-chip multidimensional fiber communications using an 8×8 triangular unitary optical mesh [63] as shown in Fig. 5(c). The minimum peak coupling efficiencies for all the six fibers mode in a two-mode FMF is about -6.1 dB. A modal crosstalk less than -21.3 dB can be achieved in our experiment. We demonstrated 32 Gbps non-return-to zero (NRZ) signal transmission across six LP modal channels, showing its ability to address multidimensional interconnect challenges with low latency and high-speed fiber communications.

C. Summary

In contrast to the GC array approach, our method optimally utilizes the excitation region, significantly enhancing the mode field overlap integral and coupling efficiency. Furthermore, when compared to the blazing grating structure [42], it allows for a substantial increase in the minimum required feature size, which can reduce the fabrication complexity. Currently, silica or 3D-waveguides based edge coupling solutions have demonstrated high efficiency exceeding -2.5 dB across all supported modes with a 1-dB bandwidth ranging from 100 to 200 nm. However, additional fabrication steps to polish the chip edge facets and a precise assembling process may be needed, hindering their cost-effective mass production. While GC-based solutions typically provide advantages in fabrication and packaging, a single 2DGC typically achieves ≤ -4 dB efficiency with <20 nm 1-dB bandwidth, thereby limiting their compatibility with WDM techniques.

Fig. 6 compares the number of spatial and polarization modes and the minimum coupling efficiency of the integrated multiplexers on a single SOI platform. Our approach achieves the highest number of selective mode excitation on a single SOI platform, while maintaining competitive coupling efficiency greater than -5.5 dB. Our proposed method for multi-mode excitation shows strong potential as a next-generation multidimensional chip-to-fiber interface. Additionally, with the development of these integrated (de)multiplexers, multidimensional optical communication in optical fibers and free-space become feasible. On-chip reconfigurable photonic meshes enable diverse management of modes and polarizations, paving the way for high-dimensional, low-latency chip-to-chip interconnect systems.

III. Discussion and Perspectives

The manipulation of various DoF of light has long been a research focus. Multidimensional chip-to-fiber I/O provide an effective approach to access various dimensions of light by planar photonic chip for reconfigurable manipulation and processing. This approach can leverage multidimensional multiplexing for various applications particularly in high-performance optical interconnects. Our demonstrate 2D grating coupler exhibits several advantages, including placement flexibility, ultra-compact footprint, competitive efficiency, while supporting up to eight spatial and polarization channels via a single I/O device. In the following we will discuss the challenges associated with our approach, future development and their impact on emerging applications.

A. Limitation

For consideration of link power budget and signal to noise ratio, enhanced coupling efficiency, optical bandwidth and increased number of multiplexed physical channels will represent the development trend for multidimensional chip-to-fiber I/O. The (de)multiplexers discussed in Section II still exhibit trade-offs among efficiency, channel count, and implementation complexity and cost.

1) Coupling Efficiency: Although our proposed diffraction gratings offer placement flexibility to form high-order spatial and polarization modes, their coupling efficiencies still needs improvements and optical bandwidth lags behind the edge-coupler-based solutions. To solve the coupling efficiency limitation, additional dielectric overlay can be applied on top of grating region to break the vertical symmetry, such as polycrystalline silicon (poly-Si) or silicon nitride (Si_3N_4) as reporeted in previous works for 1DGC [69], [71], [72], [73], [74], [75]. 2DGCs with overlay enhancement has also been investigated in simulation, where phase matching conditions should be satisfied to avoid distortion of the upward-propagating wavefront in the two orthogonal polarizations [76], [77], [78]. An experimental peak efficiency of -2.5 dB was first reported recently as a polarization-splitting 2D grating[78]. In addition, our recent work has also demonstrated poly-Si overlay can be applied for multimode 2DGC while maintaining its wavefront for the high-order modes [70]. Peak experimental coupling efficiencies can be further enhanced at the cost of additional fabrication steps. In the future, layer thickness can also be optimized to further enhance the chip-to-fiber efficiency. In terms of optical bandwidth, edge couplers exhibit superior performance compared

to grating couplers. The coupling insertion loss can be further minimized by addressing mode field mismatches and alignment offsets between silicon waveguides and optical fibers. This can be achieved through specialized fabrication techniques or the use of customized fibers.

2) Number of Spatial and Polarization Channels: Apart from the optical bandwidth, increasing the number of spatial and polarization channels is essential for enhancing the interconnect capacity. The hybrid integration of WDM and MDM is expected to enable ultra-high bandwidth in the future. The optical bandwidth advantage of edge coupling facilitates broader wavelength range. Beyond LP modes, orbital angular momentum (OAM) modes have also demonstrated potential for optical interconnects [79]. The primary challenge in generating OAM modes lies in the control of the helical phase front. Recent studies have employed star couplers and circularly arranged 2DGC arrays to manipulate spatial phase distributions, enabling the (de)multiplexing of OAM modes up to ± 11 orders [80]. Other works demonstrated hybrid multiplexing of ± 3-order OAM modes across eight wavelengths [81]. Despite their potential, OAM-based interconnects rely on specialized fibers (e.g., ring-core fibers), and their transceiver/receiver systems remain underdeveloped, which require further investigation.

B. Impact and Future Vision

Beyond optical fiber communications, the ability of multidimensional I/O to manipulate optical fields has a wide range of applications, such as:

1) Free-space optical communication: Our proposed multidimensional integrated (de)multiplexer can also be applied in free-space-to-chip coupling, where the absence of fiber constraints allows the use of any orthogonal modes and polarizations for communication. Adaptive on-chip MIMO systems hold significant promise for compensating wavefront distortions during propagation. These advancements are expected to play a crucial role in the development of next-generation high-performance freep-space optical communications.

2) Beam Shaping and Steering: The (de)multiplexer mentioned in Section 2 offers versatile control of structured light (e.g., Hermite-Gaussian (HG) beam, Laguerre-Gaussian (LG) beam, Bessel beam, Mathieu beam, etc.) by modulating the distributions of phase, intensity, and polarization [82]. Ref. [83] has advanced structured light applications by integrating a 4×4 grating array with binary-tree networks, enabling the coherent synthesis of higher-order HG and LG beams in far-field regimes. In imaging systems, the use of structured light can break through the diffraction limit and provide more detailed information by recovering high-dimensional DoF signals, enabling super-resolution imaging and 3D object reconstruction [84]. Additionally, specific high-dimensional structured light can create optical trapping, allowing for precise particle manipulation in applications such as sorting, biological assays, and material characterization [85].

3) Sensing and Spectroscopy: Different optical modes exhibit distinct responses in terms of wavelength, polarization, and phase delay to variations in pressure, temperature, concentration, etc. By detecting distortions in high-dimensional optical fields, environmental changes and structural deformations can be monitored. Additionally, as light propagates through the optical fiber, each mode experiences different changes in its wavelength information, and inter-modal interference causes spectral overlap at the output port. By analyzing multi-mode signals using PIC-MIMO technology, the original spectral characteristics can be effectively reconstructed.

4) Quantum Communication: By utilizing different modes in FMFs, multidimensional I/O can facilitate the generation and reception of entangled quantum states, which is essential for quantum key distribution (QKD) and entanglement sharing. The manipulation of high-dimensional modes, as discussed in [86], enhances the resilience of quantum communication networks to noise and turbulence, making it a promising approach for building more robust and scalable quantum networks.

IV. Conclusion

In this work, we have reported a novel multidimensional integrated (de)multiplexer on silicon for FMF. Our proposed multidimensional I/O has an ultra-compact footprint of $35 \times 35\ \mu\mathrm{m}^2$, and can efficiently and selectively launch eight LP fiber modes, including LP_{01}, LP_{11a}, LP_{11b}, and LP_{21b} in a four-mode FMF. By integrating a reconfigurable optical MZI mesh with our proposed device, spatial and polarization multiplexed optical fiber communications can be facilitated. In addition, we reviewed recent advancements in multidimensional chip-to-fiber devices and multidimensional optical systems using integrated optics from other research groups, highlighting their potential impact and applications in the next-generation optical communications, beam steering, sensing, and quantum communications.

References

[1] C. A. Brackett, "Dense wavelength division multiplexing networks: Principles and applications," *IEEE J. Sel. Areas Commun.*, vol. 8, no. 6, pp. 948–964, Aug. 1990.
[2] R. D. Feldman, E. Harstead, S. Jiang, T. H. Wood, and M. Zirngibl, "An evaluation of architectures incorporating wavelength division multiplexing for broad-band fiber access," *J. Lightw. Technol.*, vol. 16, no. 9, pp. 1546–1559, 1998.
[3] K. Hosseini et al., "8 tbps co-packaged FPGA and silicon photonics optical IO," in *Proc. Opt. Fiber Commun. Conf. Exhib.*, 2021, pp. 1–3.
[4] D. J. Richardson, J. M. Fini, and L. E. Nelson, "Space-division multiplexing in optical fibres," *Nature Photon.*, vol. 7, no. 5, pp. 354–362, 2013.
[5] P. J. Winzer, "Making spatial multiplexing a reality," *Nature Photon.*, vol. 8, no. 5, pp. 345–348, 2014.
[6] B. J. Puttnam, G. Rademacher, and R. S. Luís, "Space-division multiplexing for optical fiber communications," *Optica*, vol. 8, no. 9, pp. 1186–1203, 2021.
[7] G. Rademacher et al., "Peta-bit-per-second optical communications system using a standard cladding diameter 15-mode fiber," *Nature Commun.*, vol. 12, no. 1, 2021, Art. no. 4238.
[8] J. Liu et al., "1-Pbps orbital angular momentum fibre-optic transmission," *Light, Sci. Appl.*, vol. 11, no. 1, 2022, Art. no. 202.
[9] M. V. D. Hout et al., "Transmission of 273.6 tb/s over 1001 km of 15-mode multi-mode fiber using C-band only 16-QAM signals," *J. Lightw. Technol.*, vol. 42, no. 3, pp. 1136–1142, 2024.
[10] G. Labroille, B. Denolle, P. Jian, P. Genevaux, N. Treps, and J.-F. Morizur, "Efficient and mode selective spatial mode multiplexer based on multiplane light conversion," *Opt. Exp.*, vol. 22, no. 13, pp. 15599–15607, 2014.

[11] N. K. Fontaine, R. Ryf, H. Chen, D. T. Neilson, K. Kim, and J. Carpenter, "Laguerre-Gaussian mode sorter," *Nature Commun.*, vol. 10, no. 1, 2019, Art. no. 1865.

[12] J. Oh et al., "Adjoint-optimized metasurfaces for compact mode-division multiplexing," *ACS Photon.*, vol. 9, no. 3, pp. 929–937, 2022.

[13] R. Chen, Y.-K. Chang, Z.-P. Zhuang, Y. Liu, W.-J. Chen, and J.-W. Dong, "Metasurface-based fiber-to-chip multiplexing coupler," *Adv. Opt. Materials*, vol. 11, no. 6, 2023, Art. no. 2202317.

[14] A. Velazquez-Benitez et al., "Six mode selective fiber optic spatial multiplexer," *Opt. Lett.*, vol. 40, no. 8, pp. 1663–1666, 2015.

[15] S. Gross, N. Riesen, J. D. Love, and M. J. Withford, "Three-dimensional ultra-broadband integrated tapered mode multiplexers," *Laser Photon. Rev.*, vol. 8, no. 5, pp. L81–L85, 2014.

[16] R. Ryf et al., "Mode-division multiplexing over 96 km of few-mode fiber using coherent 6 × 6 MIMO processing," *J. Lightw. Technol.*, vol. 30, no. 4, pp. 521–531, 2012.

[17] P. J. Winzer and G. J. Foschini, "MIMO capacities and outage probabilities in spatially multiplexed optical transport systems," *Opt. Exp.*, vol. 19, no. 17, pp. 16680–16696, 2011.

[18] S. Ö. Arik, D. Askarov, and J. M. Kahn, "Effect of mode coupling on signal processing complexity in mode-division multiplexing," *J. Lightw. Technol.*, vol. 31, no. 3, pp. 423–431, 2013.

[19] P. Cheben, R. Halir, J. H. Schmid, H. A. Atwater, and D. R. Smith, "Sub-wavelength integrated photonics," *Nature*, vol. 560, no. 7720, pp. 565–572, 2018.

[20] J. Xiang et al., "Metamaterial-enabled arbitrary on-chip spatial mode manipulation," *Light, Sci. Appl.*, vol. 11, no. 1, 2022, Art. no. 168.

[21] Y. Liu et al., "Arbitrarily routed mode-division multiplexed photonic circuits for dense integration," *Nature Commun.*, vol. 10, no. 1, 2019, Art. no. 3263.

[22] J. M. Luque-González et al., "An ultracompact GRIN-lens-based spot size converter using subwavelength grating metamaterials," *Laser Photon. Rev.*, vol. 13, no. 11, 2019, Art. no. 1900172.

[23] Z. Zhang, Y. Tong, Y. Wang, and H. K. Tsang, "Nonparaxial mode-size converter using an ultracompact metamaterial mikaelian lens," *J. Lightw. Technol.*, vol. 39, no. 7, pp. 2077–2083, 2020.

[24] K. Van Acoleyen, H. Rogier, and R. Baets, "Two-dimensional optical phased array antenna on silicon-on-insulator," *Opt. Exp.*, vol. 18, no. 13, pp. 13655–13660, 2010.

[25] D. A. Miller, "Self-aligning universal beam coupler," *Opt. Exp.*, vol. 21, no. 5, pp. 6360–6370, 2013.

[26] Y. Ding et al., "Reconfigurable SDM switching using novel silicon photonic integrated circuit," *Sci. Reports*, vol. 6, no. 1, 2016, Art. no. 39058.

[27] J. Bütow et al., "Spatially resolving amplitude and phase of light with a reconfigurable photonic integrated circuit," *Optica*, vol. 9, no. 8, pp. 939–946, 2022.

[28] J. Sun, E. Timurdogan, A. Yaacobi, E. S. Hosseini, and M. R. Watts, "Large-scale nanophotonic phased array," *Nature*, vol. 493, no. 7431, pp. 195–199, 2013.

[29] D. Yi, X. Zhou, and H. K. Tsang, "Dynamic control of distal spatial mode pattern output from multimode fiber using integrated coherent network," *IEEE Photon. J.*, vol. 15, no. 5, pp. 1–5, Oct. 2023.

[30] D. Taillaert, H. Chong, P. I. Borel, L. H. Frandsen, R. M. D. L. Rue, and R. Baets, "A compact two-dimensional grating coupler used as a polarization splitter," *IEEE Photon. Technol. Lett.*, vol. 15, no. 9, pp. 1249–1251, Sep. 2003.

[31] F. Van Laere, W. Bogaerts, P. Dumon, G. Roelkens, D. Van Thourhout, and R. Baets, "Focusing polarization diversity grating couplers in silicon-on-insulator," *J. Lightw. Technol.*, vol. 27, no. 5, pp. 612–618, 2009.

[32] J. Zou, Y. Yu, and X. Zhang, "Single step etched two dimensional grating coupler based on the SOI platform," *Opt. Exp.*, vol. 23, no. 25, pp. 32490–32495, 2015.

[33] C. Lacava et al., "Design and characterization of low-loss 2D grating couplers for silicon photonics integrated circuits," *Proc. SPIE*, vol. 9752, 2016, Art. no. 97520V.

[34] T. Watanabe, Y. Fedoryshyn, and J. Leuthold, "2-D grating couplers for vertical fiber coupling in two polarizations," *IEEE Photon. J.*, vol. 11, no. 4, pp. 1–9, Aug. 2019.

[35] B. Chen et al., "Two-dimensional grating coupler on silicon with a high coupling efficiency and a low polarization-dependent loss," *Opt. Exp.*, vol. 28, no. 3, pp. 4001–4009, 2020.

[36] N. K. Fontaine et al., "Space-division multiplexing and all-optical MIMO demultiplexing using a photonic integrated circuit," in *Proc. OFC/NFOEC*, 2012, pp. 1–3.

[37] S. B. Yoo, R. P. Scott, D. J. Geisler, N. K. Fontaine, and F. M. Soares, "Terahertz information and signal processing by RF-photonics," *IEEE Trans. Terahertz Sci. Technol.*, vol. 2, no. 2, pp. 167–176, Mar. 2012.

[38] A. Koonen, H. Chen, H. P. van den Boom, and O. Raz, "Silicon photonic integrated mode multiplexer and demultiplexer," *IEEE Photon. Technol. Lett.*, vol. 24, no. 21, pp. 1961–1964, Nov. 2012.

[39] Y. Ding, H. Ou, J. Xu, and C. Peucheret, "Silicon photonic integrated circuit mode multiplexer," *IEEE Photon. Technol. Lett.*, vol. 25, no. 7, pp. 648–651, Apr. 2013.

[40] B. Wohlfeil, G. Rademacher, C. Stamatiadis, K. Voigt, L. Zimmermann, and K. Petermann, "A two-dimensional fiber grating coupler on SOI for mode division multiplexing," *IEEE Photon. Technol. Lett.*, vol. 28, no. 11, pp. 1241–1244, Jun. 2016.

[41] Y. Tong, W. Zhou, X. Wu, and H. K. Tsang, "Efficient mode multiplexer for few-mode fibers using integrated silicon-on-insulator waveguide grating coupler," *IEEE J. Quantum Electron.*, vol. 56, no. 1, pp. 1–7, Feb. 2020.

[42] T. Watanabe, B. I. Bitachon, Y. Fedoryshyn, B. Baeuerle, P. Ma, and J. Leuthold, "Coherent few mode demultiplexer realized as a 2D grating coupler array in silicon," *Opt. Exp.*, vol. 28, no. 24, pp. 36009–36019, 2020.

[43] W. Zhou, Z. Zhang, H. Chen, H. K. Tsang, and Y. Tong, "Ultra-compact and efficient integrated multichannel mode multiplexer in silicon for few-mode fibers," *Laser Photon. Rev.*, vol. 18, no. 4, 2024, Art. no. 2300460.

[44] W. Shen, J. Du, J. Xiong, L. Ma, and Z. He, "Silicon-integrated dual-mode fiber-to-chip edge coupler for 2× 100 gbps/lambda MDM optical interconnection," *Opt. Exp.*, vol. 28, no. 22, pp. 33254–33262, 2020.

[45] K. Y. Yang et al., "Multi-dimensional data transmission using inverse-designed silicon photonics and microcombs," *Nature Commun.*, vol. 13, no. 1, 2022, Art. no. 7862.

[46] O. A. J. Gordillo et al., "Fiber-chip link via mode division multiplexing," *IEEE Photon. Technol. Lett.*, vol. 35, no. 19, pp. 1071–1074, Oct. 2023.

[47] X. Cao, K. Li, Y. Wan, and J. Wang, "Efficient mode coupling between a few-mode fiber and multi-mode photonic chip with low crosstalk," *Opt. Exp.*, vol. 30, no. 13, pp. 22637–22648, 2022 .

[48] X. Yi, W. Zhao, Y. Shi, and D. Dai, "Novel concept of high-efficiency coupling between silicon photonic chips and few-mode-fibers," in *Proc. 2022 Asia Commun. Photon. Conf.*, 2022, pp. 1600–1602.

[49] R. Zhang et al., "Ultra-high bandwidth density and power efficiency chip-to-chip multimode transmission through a rectangular core few-mode fiber," *Laser Photon. Rev.*, vol. 17, no. 11, 2023, Art. no. 2200750.

[50] J. Wang, S. He, and D. Dai, "On-chip silicon 8-channel hybrid (de) multiplexer enabling simultaneous mode-and polarization-division-multiplexing," *Laser Photon. Rev.*, vol. 8, no. 2, pp. L18–L22, 2014.

[51] J. Xing, Z. Li, X. Xiao, J. Yu, and Y. Yu, "Two-mode multiplexer and demultiplexer based on adiabatic couplers," *Opt. Lett.*, vol. 38, no. 17, pp. 3468–3470, 2013.

[52] D. Dai and H. Wu, "Realization of a compact polarization splitter-rotator on silicon," *Opt. Lett.*, vol. 41, no. 10, pp. 2346–2349, 2016.

[53] K. Li, X. Cao, and J. Wang, "Broadband and efficient multi-mode fiber-chip edge coupler on a silicon platform assisted with a nano-slot waveguide," *Opt. Exp.*, vol. 30, no. 26, pp. 47249–47263, 2022.

[54] B. Guan et al., "Polarization diversified integrated circuits for orbital angular momentum multiplexing," in *Proc. IEEE Photon. Conf.*, 2015, pp. 649–652.

[55] C. Antonelli, A. Mecozzi, M. Shtaif, and P. J. Winzer, "Nonlinear propagation equations in fibers with multiple modes—Transitions between representation bases," *APL Photon.*, vol. 4, no. 2, 2019, pp. 228061–228067.

[56] X. Chen, C. Li, and H. K. Tsang, "Fabrication-tolerant waveguide chirped grating coupler for coupling to a perfectly vertical optical fiber," *IEEE Photon. Technol. Lett.*, vol. 20, no. 23, pp. 1914–1916, Dec. 2008.

[57] Y. Tong, W. Zhou, and H. K. Tsang, "Efficient perfectly vertical grating coupler for multi-core fibers fabricated with 193 nm DUV lithography," *Opt. Lett.*, vol. 43, no. 23, pp. 5709–5712, 2018.

[58] X. Yi, W. Zhao, L. Zhang, Y. Shi, and D. Dai, "Efficient mode coupling/(de) multiplexing between a few-mode fiber and a silicon photonic chip," *Photon. Res.*, vol. 12, no. 12, pp. 2784–2793, 2024.

[59] Y. Wan et al., "Multidimensional fiber-to-chip optical processing using photonic integrated circuits," *Laser Photon. Rev.*, vol. 18, no. 9, 2024, Art. no. 2300853.

[60] K. Li et al., "Fiber–chip–fiber mode/polarization/wavelength transmission and processing with few-mode fiber,(de) multiplexing SiO2 chip and ROADM Si chip," *Laser Photon. Rev.*, vol. 18, no. 7, 2024, Art. no. 2300489.

[61] S. SeyedinNavadeh et al., "Determining the optimal communication channels of arbitrary optical systems using integrated photonic processors," *Nature Photon.*, vol. 18, no. 2, pp. 149–155, 2024.
[62] B. Wu et al., "Chip-to-chip optical multimode communication with universal mode processors," *PhotoniX*, vol. 4, no. 1, 2023, Art. no. 37.
[63] K. Lu et al., "Empowering high-dimensional optical fiber communications with integrated photonic processors," *Nature Commun.*, vol. 15, no. 1, 2024, Art. no. 3515.
[64] D. A. Miller, "Establishing optimal wave communication channels automatically," *J. Lightw. Technol.*, vol. 31, no. 24, pp. 3987–3994, 2013.
[65] A. Annoni et al., "Unscrambling light—automatically undoing strong mixing between modes," *Light, Sci. Appl.*, vol. 6, no. 12, pp. e17110–e17110, 2017.
[66] R. Tang et al., "Reconfigurable all-optical on-chip MIMO three-mode demultiplexing based on multi-plane light conversion," *Opt. Lett.*, vol. 43, no. 8, pp. 1798–1801, 2018.
[67] M. Milanizadeh et al., "Separating arbitrary free-space beams with an integrated photonic processor," *Light: Sci. Appl.*, vol. 11, no. 1, 2022, Art. no. 197.
[68] W. Bogaerts et al., "Programmable photonic circuits," *Nature*, vol. 586, no. 7828, pp. 207–216, 2020.
[69] X. Zhou and H. K. Tsang, "High efficiency multimode waveguide grating coupler for few-mode fibers," *IEEE Photon. J.*, vol. 14, no. 4, pp. 1–5, Aug. 2022.
[70] W. Zhou et al., "Efficient and adaptive reconfiguration of light structure in optical fibers with programmable silicon photonics," *Optica*, vol. 12, no. 3, pp. 329–336, 2025.
[71] W. D. Sacher et al., "Monolithically integrated multilayer silicon nitride-on-silicon waveguide platforms for 3-D photonic circuits and devices," *Proc. IEEE*, vol. 106, no. 12, pp. 2232–2245, Dec. 2018.
[72] C. Qiu et al., "Poly-silicon grating couplers for efficient coupling with optical fibers," *IEEE Photon. Technol. Lett.*, vol. 24, no. 18, pp. 1614–1617, Sep. 2012.
[73] G. Roelkens et al., "High efficiency diffractive grating couplers for interfacing a single mode optical fiber with a nanophotonic silicon-on-insulator waveguide circuit," *Appl. Phys. Lett.*, vol. 92, no. 13, 2008, pp. 1–3.
[74] Y. Tong, X. Zhou, Y. Wang, C.-W. Chow, and H. K. Tsang, "Bridging the graded-index few-mode fibre with photonic integrated circuits via efficient diffraction waveguide gratings," in *Proc. Eur. Conf. Integr. Opt.*, 2020, pp. 1311011–1311013.
[75] V. Vitali et al., "High-efficiency reflector-less dual-level silicon photonic grating coupler," *Photon. Res.*, vol. 11, no. 7, pp. 1275–1283, 2023.
[76] L. Carroll, D. Gerace, I. Cristiani, and L. C. Andreani, "Optimizing polarization-diversity couplers for Si-photonics: Reaching the- 1dB coupling efficiency threshold," *Opt. Exp.*, vol. 22, no. 12, pp. 14769–14781, 2014.
[77] X. Zhou and H. K. Tsang, "High efficiency polarization-diversity two-dimensional waveguide grating coupler for perfectly vertical coupling," in *Proc. IEEE Silicon Photon. Conf.*, 2024, pp. 1–2.
[78] W. Zhou, K. Lu, S. Kang, X. Wu, and Y. Tong, "Efficient polarization-diversity grating coupler with multipolar radiation mode enhancement," *IEEE Photon. J.*, vol. 17, no. 2, pp. 1–6, Apr. 2025.
[79] H. Song et al., "Free-space optical communication link using a single Laguerre-Gaussian beam with tunable radial and azimuthal spatial indices generated by an integrated concentric circular antenna array," *Opt. Exp.*, vol. 32, no. 19, pp. 33803–33810, 2024.
[80] Y. Chen, S. Levasseur, L. A. Rusch, and W. Shi, "Integrated phased array for scalable vortex beam multiplexing," *J. Lightw. Technol.*, vol. 41, no. 7, pp. 2070–2078, 2022.
[81] Y. Chen, Z. Lin, S. Belanger-de Villers, L. A. Rusch, and W. Shi, "WDM-compatible polarization-diverse OAM generator and multiplexer in silicon photonics," *IEEE J. Sel. Top. Quantum Electron.*, vol. 26, no. 2 Mar./Apr. 2020, Art. no. 6100107.
[82] J. Wang, K. Li, and Z. Quan, "Integrated structured light manipulation," *Photon. Insights*, vol. 3, no. 3, pp. R05–R05, 2024.
[83] J. Bütow, J. S. Eismann, V. Sharma, D. Brandmüller, and P. Banzer, "Generating free-space structured light with programmable integrated photonics," *Nature Photon.*, vol. 18, no. 3, pp. 243–249, 2024.
[84] P. Song et al., "Super-resolution microscopy via ptychographic structured modulation of a diffuser," *Opt. Lett.*, vol. 44, no. 15, pp. 3645–3648, 2019.
[85] A. Kritzinger, A. Forbes, and P. B. Forbes, "Optical trapping and fluorescence control with vectorial structured light," *Sci. Reports*, vol. 12, no. 1, 2022, Art. no. 17690.
[86] Y. Zheng et al., "Multichip multidimensional quantum networks with entanglement retrievability," *Science*, vol. 381, no. 6654, pp. 221–226, 2023.